N87-11219

TURBINE AIRFOIL GAS SIDE HEAT TRANSFER*

Edward R. Turner

Allison Gas Turbine Division
General Motors Corporation

ABSTRACT

Work is currently underway to develop and characterize an analytical approach, based on boundary layer theory, for predicting the effects of leading edge (showerhead) film cooling on downstream gas side heat transfer rates. Parallel to this work, experiments are being conducted to build a relevant data base for present and future methods verification.

INTRODUCTION

In a previous work (NAS3-22761), the emphasis was placed on developing more accurate analytical models for predicting local gas side heat transfer rates on modern non-film-cooled turbine vane geometries. Analytical and experimental results of that program are detailed in Reference 1. However, it is recognized that as future core turbine designs move towards higher turbine inlet temperatures, some degree of surface film cooling will be required to meet projected performance and durability goals. Therefore, the purpose of this work is to initiate an in-depth analytical/experimental characterization of heat transfer phenomena associated with film cooling by first considering a specific film cooling configuration commonly used in practice.

In particular, it has been demonstrated that multiple hole (showerhead) film cooling of the critical vane leading edge region can significantly enhance the long-term durability of vanes which otherwise are internally cooled by combination of convection and jet impingement techniques. While experiments and analyses have been reported that address the heat transfer problem within the showerhead array itself (e.g., Refs 2 to 5), there has been little systematic effort aimed at characterizing local downstream effects on highly loaded airfoil surfaces operating at realistic Mach number, Reynolds number, wall-to-gas, and coolant-to-gas temperature ratios.

The primary objective of this work is to develop a designer useable analytical method for predicting local heat transfer rate differences that exist between non-film-cooled and leading edge film-cooled airfoil designs in regions downstream of the showerhead array. In support of this objective, experiments are being conducted to build a realistic data base for developing and verifying modeling assumptions.

*This work is being performed under Contract NAS3-23695.

What follows first is a summary of the completed experimental program. This is followed by a discussion of some experimental results that illustrate important physical attributes of the leading edge film-cooled heat transfer problem that are receiving the most attention in the current methods development effort. Finally, the overall analytical program is summarized in terms of general approach and remaining tasks.

EXPERIMENTAL PROGRAM

The experimental technique used for determining local heat transfer coefficient distributions downstream of a showerhead array follows exactly that used for the non-film-cooled experiments reported in Reference 1 and summarized by Figure 1. As Figure 1 illustrates, a local surface heat transfer coefficient distribution is determined by experimentally measuring steady-state aerothermal boundary conditions and then numerically solving the heat conduction equation to calculate the airfoil internal temperature distribution. Once done, a local heat transfer coefficient can be formed using locally calculated surface normal temperature gradient, measured wall and gas temperatures, and material conductivity.

The film-cooled leading edge heat transfer experiments were conducted utilizing a two-dimensional (2-D) linear cascade of three vanes. The vane profile used in this work was identical to that referred to as the C3X vane in Reference 1. The leading edge for a new C3X test vane was designed and fabricated to include five rows of staggered holes to simulate a plenum-fed showerhead array. Geometric details of the actual array are summarized in Table I. The C3X profile used in both the non-film-cooled and film-cooled experiments is shown in Figure 2. This figure also indicates that the only difference between the non-film-cooled and film-cooled leading edge vane test hardware is in the details of the leading edge region. As nearly as possible, the present film-cooled experimental program was structured to directly extend the non-film-cooled C3X data base (Ref 1) with minor changes in technique and hardware. A photograph of one-half of the actual film-cooled C3X test vane that illustrates the structural configuration of the leading edge array is shown in Figure 3.

Experiments were conducted to simulate the case where all leading edge holes are supplied by a common plenum. This reflects the situation that exists for the majority of real designs. Aerodynamic and heat transfer data were obtained at two cascade exit Mach number (M_2) levels and three exit Reynolds number (Re_2) levels. At each exit Mach number/Reynolds number operating condition, plenum coolant-to-mainstream total pressure ratio, P_c/P_t (blowing strength), and plenum coolant-to-mainstream total temperature ratio, T_c/T_g (cooling strength), were systematically varied. A total of 45 heat transfer data sets were obtained within the experimental program. The ranges of test operating conditions for the four parameters varied are summarized in Table II.

EXPERIMENTAL RESULTS

In presenting the experimental heat transfer results, the goal is to isolate the differences between non-film-cooled and leading edge film-cooled heat transfer phenomena downstream of the showerhead array. This can be accomplished by ratioing the experimentally determined local Stanton number for cases where coolant is being ejected from the leading edge to the local Stanton number determined for the case where no coolant is added.

Rather than simply form the film-cooled Stanton number-to-non-filmed-cooled Stanton number ratio (St_{FC}/St_{NFC}), which would take on values about a "no difference" value of unity, an alternate parameter referred to as Stanton number reduction (SNR) is used. SNR is defined as

$$SNR = 1 - St_{FC}/St_{NFC} \qquad (1)$$

Therefore, SNR=0 implies "no difference" and positive or negative values imply reduced or increased heat transfer levels respectively. Forming SNR values along the entire test surface gives the actual SNR distribution for the airfoil. In addition, St_{FC}/St_{NFC} is determined using data obtained at equivalent M_2 and Re_2 conditions, so SNR is approximately equal to the actual heat transfer coefficient reduction.

Figures 4 and 5 are used to illustrate the formation and type information given by vane surface SNR distributions. All data shown in these figures were obtained at fixed operating conditions; i.e., $M_2 = 0.90$, $Re_2 = 2.0 \times 10^6$, $T_c/T_g = 0.8$. Variable blowing strengths ($P_c/P_t = 1.0, 1.02, 1.05, 1.10$) were set to at these conditions and heat transfer data taken. The four different surface heat transfer coefficient distributions determined from the cascade data at the four P_c/P_t conditions are shown in Figure 4. A value of $P_c/P_t = 1.0$ signifies a no coolant ejection condition and $P_c/P_t > 1.0$ signifies coolant is being ejected. Using the results of Figure 4 and the SNR definition given by equation (1), surface SNR distributions can be constructed. These are shown in Figure 5. Since each SNR distribution only shows the difference between a given film and baseline non-film-cooled condition, a SNR data presentation is useful for discussing phenomena unique to the film-cooled problem. This can be demonstrated by concentrating on some of the more important findings of the experimental program. Note first that the SNR results in Figure 5 indicate that the major difference in heat transfer level occurs on the suction surface between 20 and 40 percent surface distance ($0.2 < S < 0.4$). This region corresponds to what is considered to be the suction surface transition zone (see Figure 4). Therefore, over the range of blowing strengths represented by the data in Figures 4 and 5, the primary effect of leading edge film cooling is to increase the pre-turbulent boundary layer heat transfer levels ($SNR < 0$).

This pre-turbulent increase is similar in character to what would be anticipated by increasing the free-stream turbulence intensity. Thus, it appears that the discrete injection process acts as a turbulence promoter and/or simulated boundary layer trip device. Although the pressure surface seems to be unaffected in view of

the results shown in Figures 4 and 5, the same suction surface phenomenon is present but only to a lesser degree. This statement is supported by the results shown in Figure 6. SNR data shown in Figure 6 were obtained at the same fixed operating conditions (M_2, Re_2, T_c/T_g) as those in Figures 4 and 5 but at higher blowing strengths (P_c/P_t = 1.3-1.7).

Figure 6 clearly illustrates the so-called pre-turbulent increase in heat transfer (SNR < 0) associated with the discrete injection process on both the suction and pressure surfaces. Quantitative differences may be explained in part by differences in surface static pressure levels and/or gradient between the two surfaces. C3X test vane measured and predicted surface static-to-inlet total pressure distributions (P_s/P_t) are shown for reference in Figure 7.

Representative SNR data, indicative of differences associated with exit Reynolds number (Re_2) variation (M_2, T_c/T_g, P_c/P_t fixed), are shown in Figure 8. The main qualitative difference in the results is the location of the zone of negative SNR (increased heat transfer) on the suction surface. Figure 8 indicates that since transition zone location changes as Reynolds number is varied, the pre-turbulent region most affected by the injection process would be shifted. The progressively earlier location of minimum suction surface SNR with increasing Reynolds number is consistent with what would be expected in terms of transition origin versus Reynolds number models. The absence of a definitive trend difference on the pressure surface suggests a less well defined (understood) transition process.

One of the questions posed prior to this work was whether there were any benefits to be extracted from leading edge injection in terms of recovery region surface protection. To partially answer this question, Figure 9 is referred to. Data shown was obtained at variable plenum coolant-to-mainstream total temperature ratios (T_c/T_g = 0.7,0.8,0.9) at fixed M_2, Re_2, P_c/P_t conditions. The general overall increase in SNR (decreased heat transfer) as T_c/T_g is decreased indicates the positive effect that results from diluting the hot free-stream fluid with the colder leading edge ejectant. However, as the pressure surface results indicate, the favorable dilution phenomenon is offset by the adverse turbulence generation mechanism associated with the discrete injection process (see Figure 5). The net result is that even for T_c/T_g = 0.7, SNR is still negative immediately downstream of the showerhead on the pressure surface.

Figure 9 also indicates that the dilution versus turbulence generation mechanisms are at work on the suction surface. However, SNR results shown in Figure 6 indicate that in the fully turbulent region (S > 0.4) no significant effect is expected (i.e., SNR ≃ 0 for S > 0.4) as a result of the leading edge injection process. Therefore, Figures 6 and 9 together support the notion that in pre-turbulent zones the SNR result obtained is governed by the competing dilution/turbulence generation mechanisms, while in the fully turbulent zones the SNR result is determined by dilution strength only. If this is the case, then it can be argued that leading edge film cooling by itself cannot be used to always offset high near recovery region heat loads even though far recovery region loads are reduced.

Finally, one curious result concerning suction surface transition behavior is illustrated in Figures 4 and 5. Studying the suction surface heat transfer coefficient data of Figure 4 first, note that transition in the thermodynamic boundary layer sense appears to complete near S = 0.6 or the location where the heat transfer coefficient appears to level off. However, SNR data of Figure 5 indicate that the upstream disturbance (leading edge discrete injection in this case) causes no change beyond S = 0.4. Therefore, it would seem that the S = 0.4 location distinctly delineates pre- and post-transition zones in terms of disturbance phenomena. But the fact that between S = 0.4 and S = 0.6 the heat transfer coefficient is still increasing (Figure 4) contradicts the above statement.

It is theorized that perhaps the apparently contradictory trends in Figures 4 and 5 actually are indicative of transition rate differences between the hydrodynamic and thermodynamic boundary layers. That is, since the SNR data of Figure 5 show the type results that would be obtained by introducing a simulated boundary layer trip, then the "no difference" result beyond S = 0.4 might imply that the untripped hydrodynamic boundary layer had completed transition near S = 0.4. However, heat transfer coefficient data of Figure 4 indicate that both the disturbed and undisturbed thermodynamic boundary layers complete transition further downstream nearer S = 0.6. Since parallel measurements of the developing hydrodynamic boundary layer state were not made (e.g., surface wall shear stress distributions), it is impossible to conclusively quantify the implied differences between hydrodynamic and thermodynamic transition phenomena suggested here.

ANALYTICAL PROGRAM

The overall objective of the analytical methods development program is to develop a computational technique, based on boundary layer theory, to predict the SNR type results shown in Figures 5, 6, 8 and/or 9. Work towards this objective is currently in progress.

The basic approach being taken is to develop a modified version of the finite difference boundary layer code, STAN5, for predicting within regions downstream of the showerhead array where it is assumed that a boundary layer would re-form. The initial task as far as this approach is concerned is to develop a method for generating appropriate starting location velocity and thermal profiles that reflect experimental results in terms of wall gradient quantities (initial location heat flux or heat transfer coefficient.) For this effort, a previously developed non-blown similarity solution technique (Refs 1 and 5) is being modified to account for the turbulence generation and dilution mechanism phenomenon associated with a discrete injection process.

Following this work, the final task will be to develop a suitable model for tracking the disturbance decay through transition. This is perhaps the more difficult problem since the success of this effort depends in part on having a reliable, undisturbed (non-blown) transition model. It can be argued that a consistently reliable, non-film-cooled airfoil transition model does not yet exist. However, if at a minimum the important qualitative trends present in the experimental results are captured, then the final prediction code will be of value to the turbine cooling designer interested in obtaining a more correct evaluation of the overall heat transfer benefits or penalties associated with leading edge film-cooled airfoil geometries.

REFERENCES

1. Hylton, L.D.; Mihelc, M.S.; Turner, E.R.; Nealy, D.A.; and York, R.E: Analytical and Experimental Evaluation of Heat Transfer Distribution Over the Surfaces of Turbine Vanes. NASA CR 168015, 1983.

2. Luckey, D.W.; and L'Ecuyer, M.R.: Stagnation Region Gas Film Cooling--Spanwise Angled Injection from Multiple Rows of Holes. NASA CR 165333, 1981.

3. Bonnice, M.A.; and L'Ecuyer, M.R.: Stagnation Region Gas Film Cooling--Effects of Dimensionless Coolant Temperature. NASA CR 168197, 1983.

4. Stepka, F.S.; and Gaugler, R.E.: Comparison of Predicted and Experimental External Heat Transfer Around a Film Cooled Cylinder in Crossflow. ASME Paper No. 83-GT-47, 1983.

5. Miller, K.L.; and Crawford, M.E: Numerical Simulation of Single, Double, and Multiple Row Film Cooling Effectiveness and Heat Transfer. ASME Paper No. 84-GT-112, 1984.

6. Kwon O.K.; Turner, E.R.; and Kou, Y.M.: Prediction of Stagnation Flow Heat Transfer on Turbomachinery Airfoils. AIAA Paper No. 83-1173, 1983.

Table I.
Film-cooled leading edge geometry.

Geometric parameters	Value
Rows of holes*	5
Hole pitch-to-diameter ratio (P/D)	4.0
Hole spacing-to-diameter ratio (S/D)	7.5
Hole slant angle (α)--deg	45
Hole skew angle (β)--deg	90

*Centered about location of maximum surface static pressure

Table II.
Range of parameters varied in film-cooled experiments.

Parameter	Range
Exit Mach number, M_2	0.90-1.05
Exit Reynolds number, Re_2	1.5×10^6-2.5×10^6
Plenum coolant-to-mainstream total pressure ratio, P_c/P_t	1.0-1.7
Plenum coolant-to-mainstream total temperature ratio, T_c/T_g	0.6-0.9

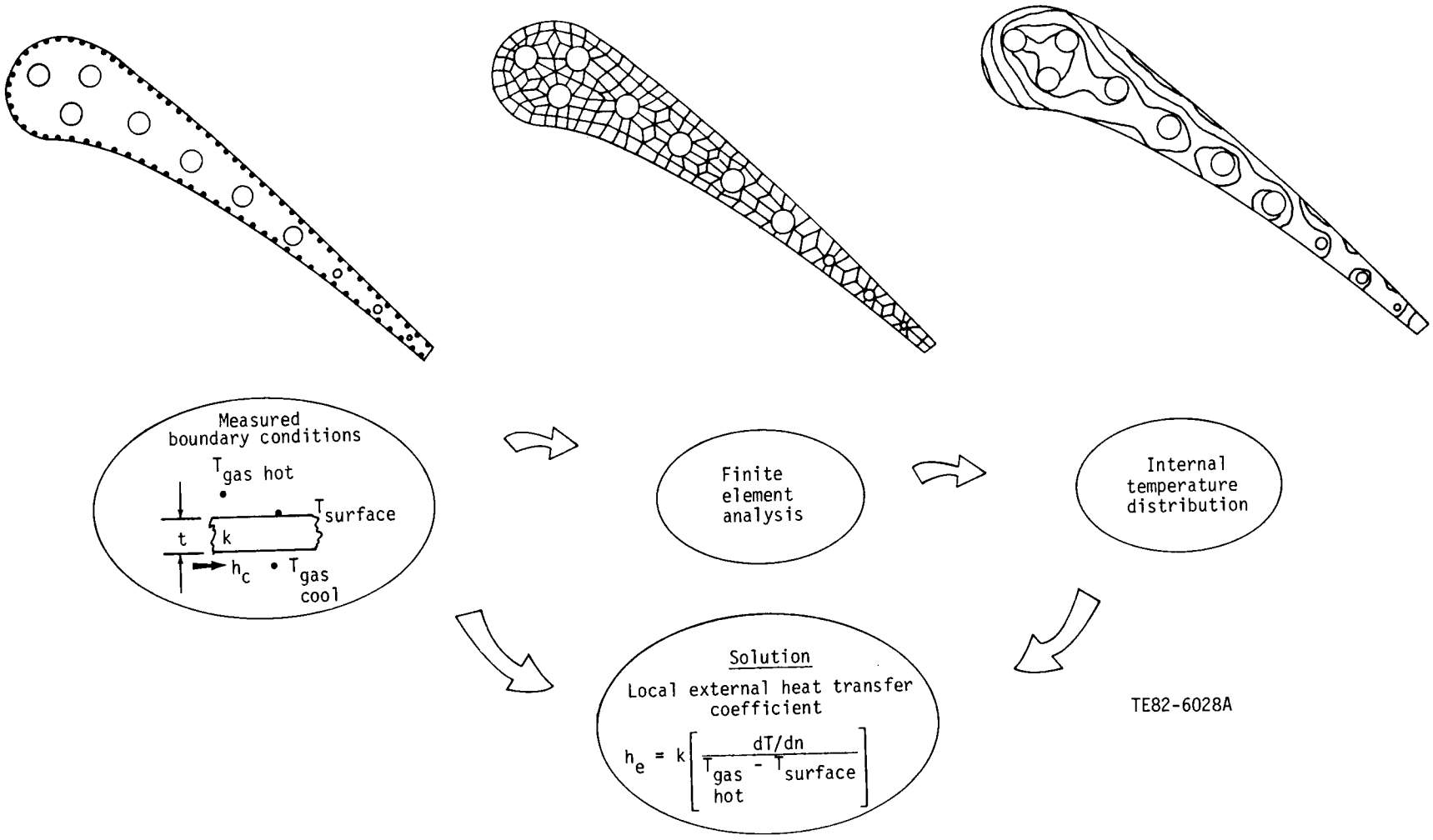

Figure 1. Heat transfer data reduction technique.

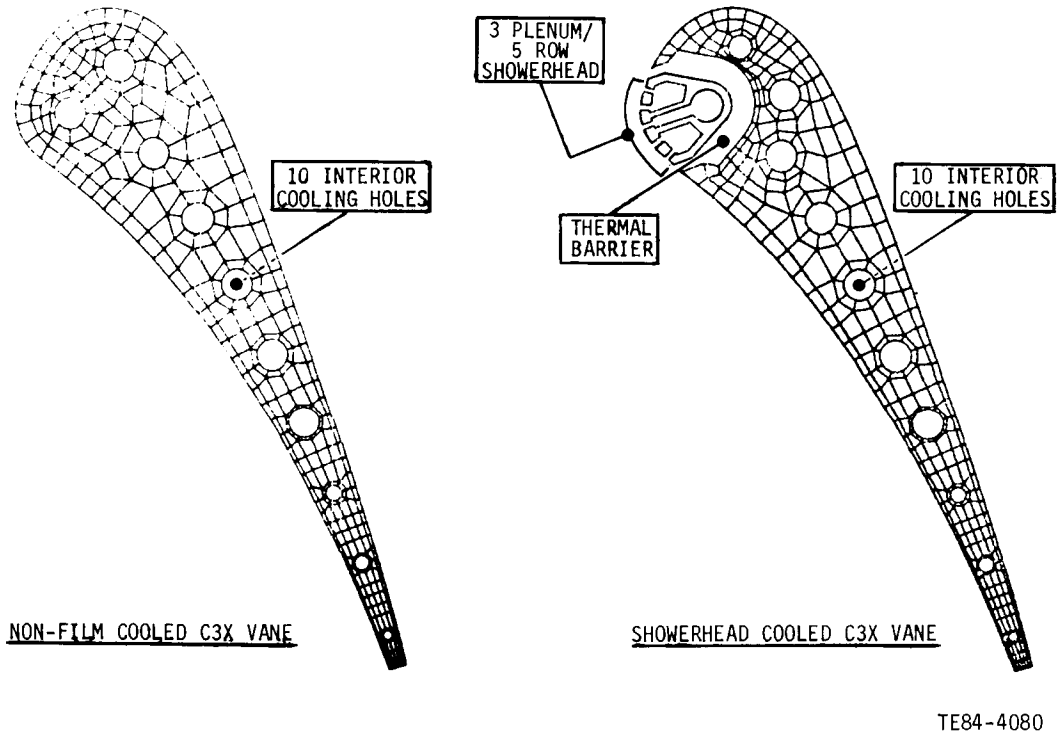

Figure 2. Cross section of C3X vanes for heat transfer experiments.

Figure 3. Film-cooled C3X vane half prior to instrumentation.

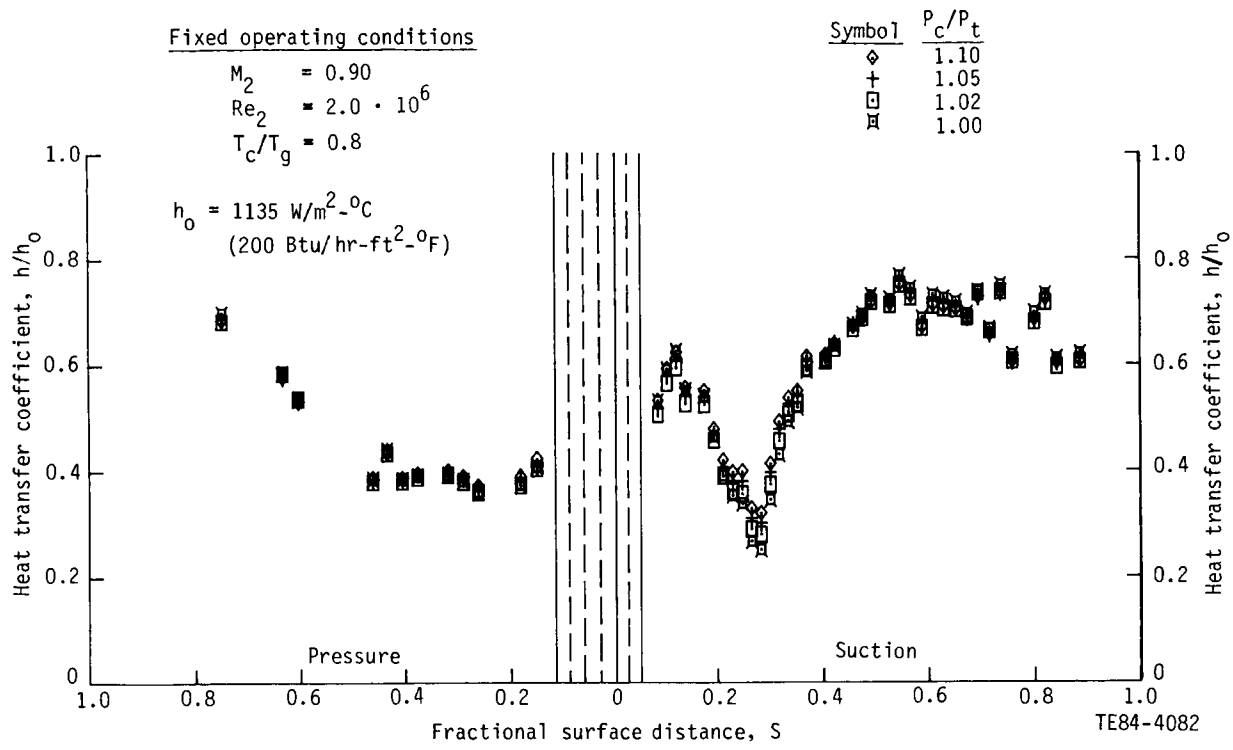

Figure 4. Variable blowing strength heat transfer coefficient data.

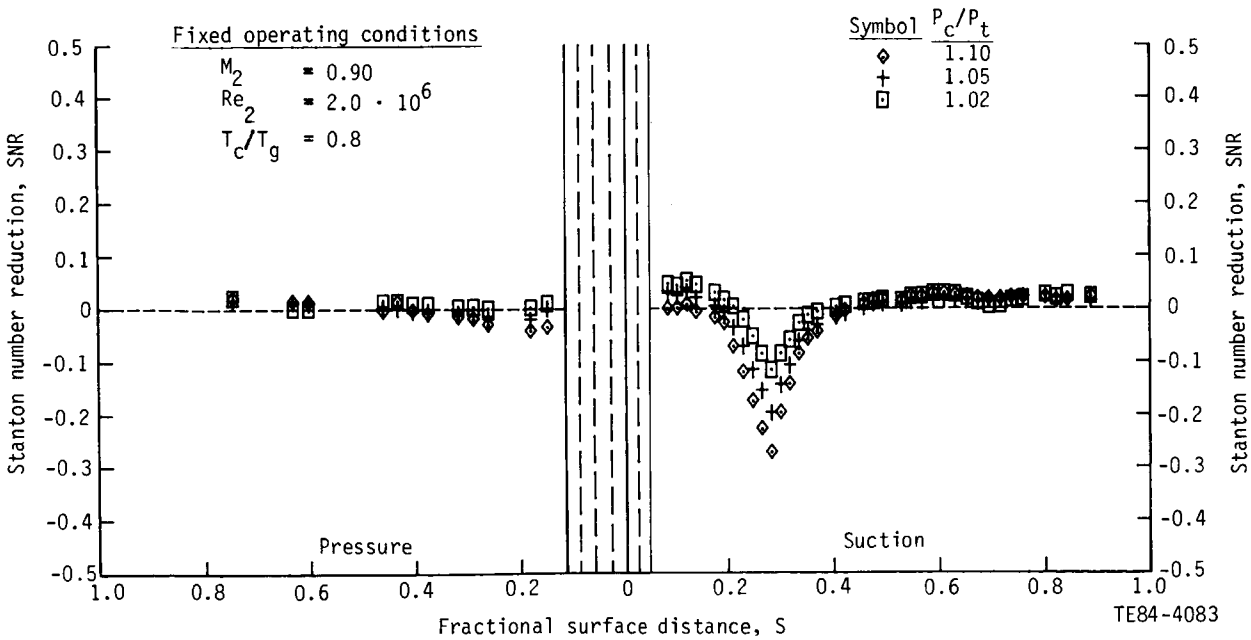

Figure 5. Effect of blowing strength variation.

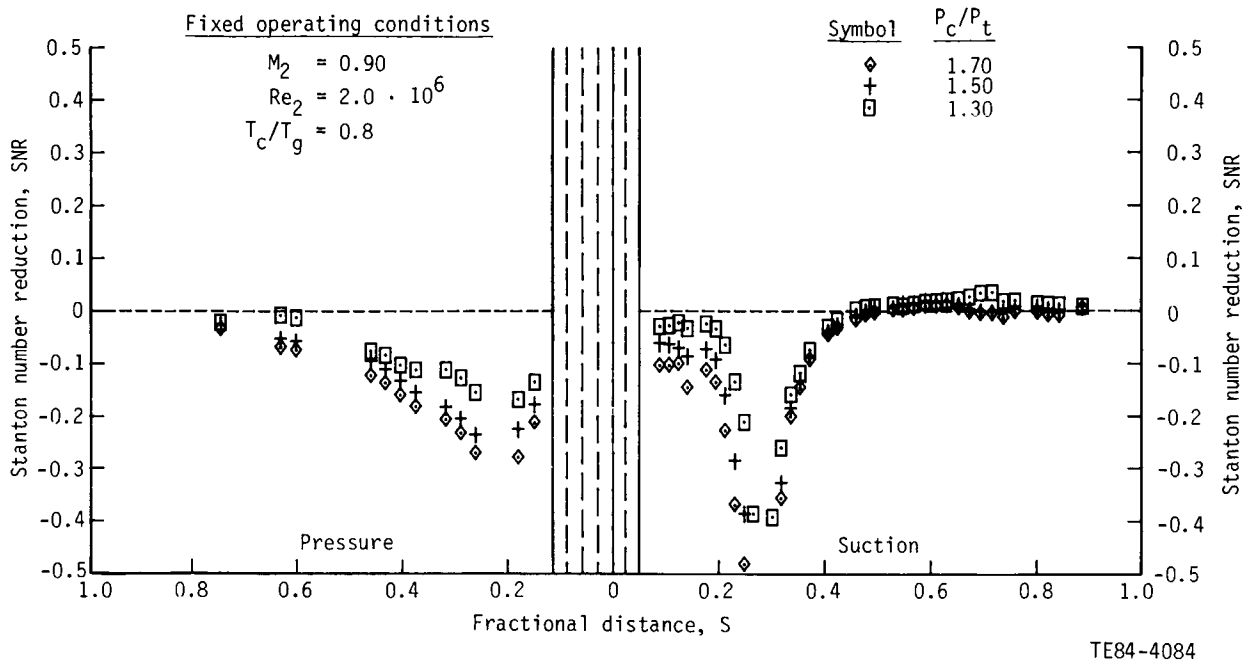

Figure 6. Effect of blowing strength variation.

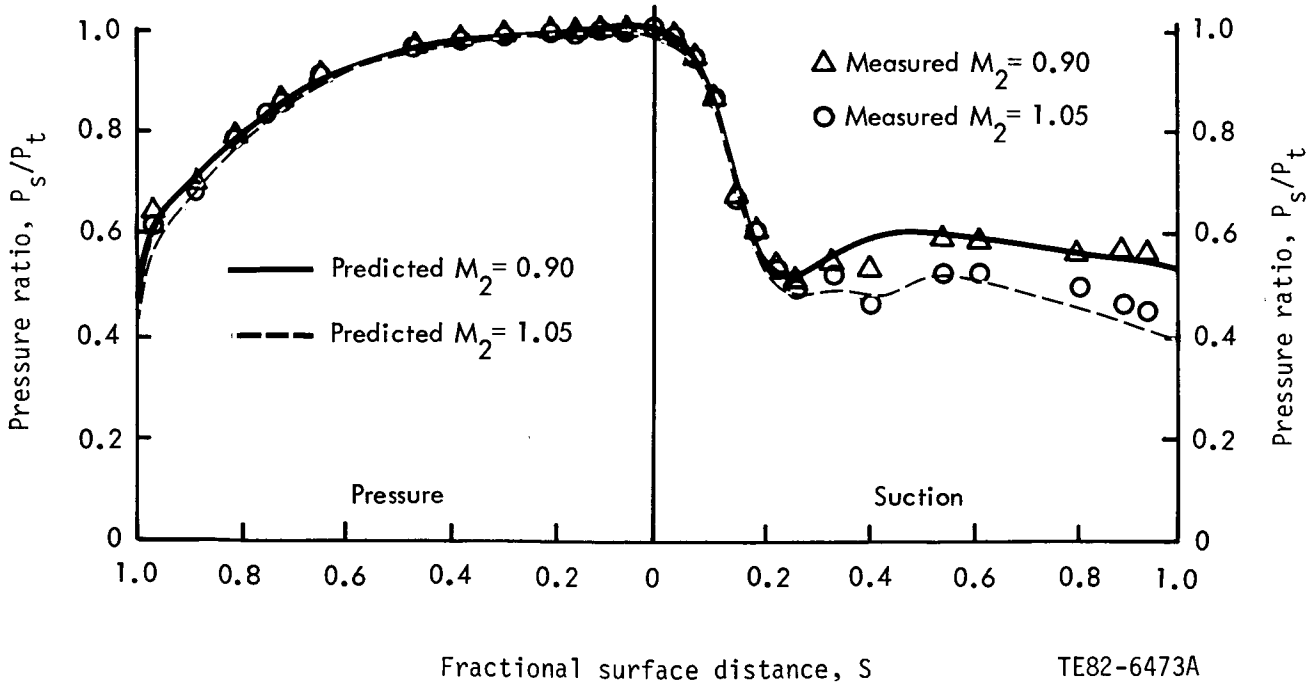

Figure 7. Surface static-to-inlet total pressure distributions.

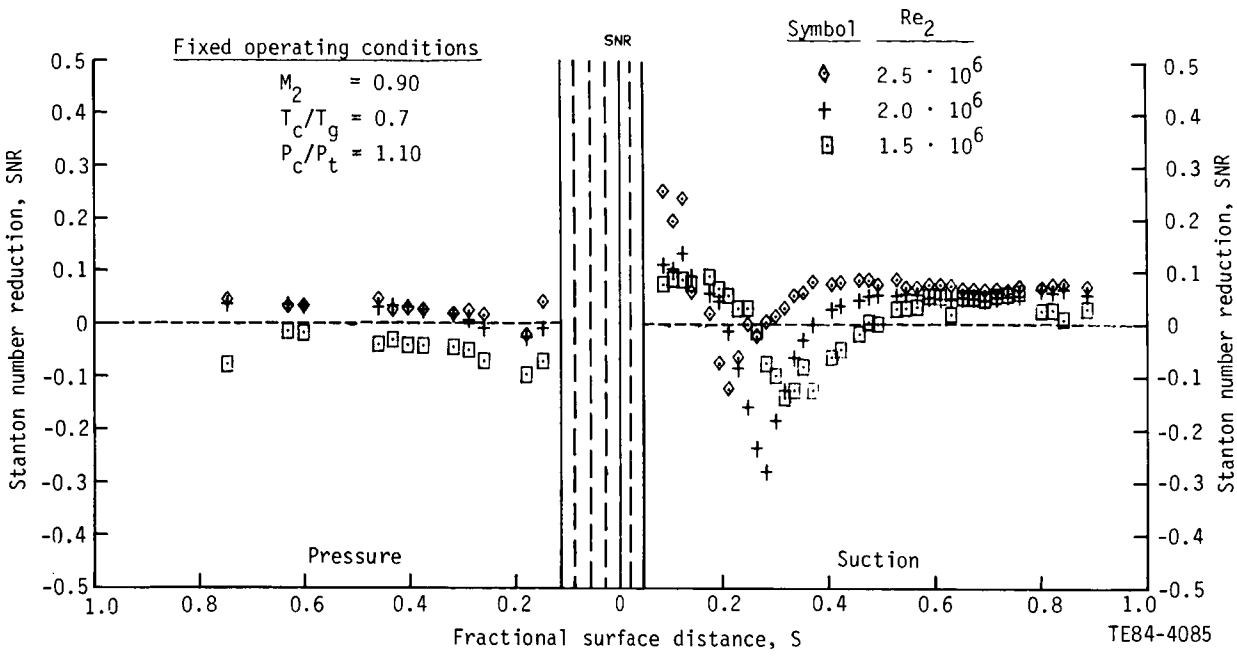

Figure 8. Effect of Reynolds number variation.

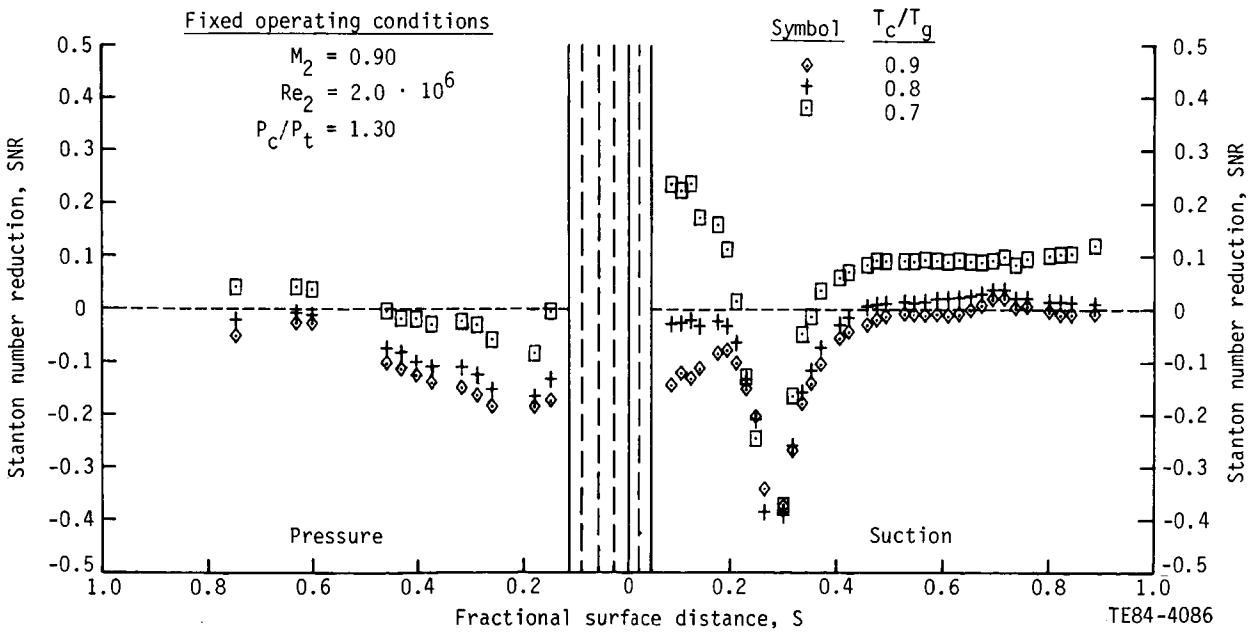

Figure 9. Effect of coolant temperature variation.